long necks and tails could have facilitated heat dissipation by increasing their surface area (*37*). Overall, our data are most consistent with the hypothesis that sauropods sustained high metabolic rates during ontogeny to reach their gigantic size so rapidly, but that in maturity a combination of physiological and behavioral adaptations and/or a slowing of metabolic rate prevented problems with overheating and avoided excessively high body temperatures (*18*, *36*). An unresolved question is whether such adaptations could have compensated for the high internal heat production associated with endothermy, or whether large adult sauropods must have had both heat-dissipating adaptations and a low basal metabolism to maintain body temperatures in the 36° to 38°C range that we have measured.

References and Notes

1. L. S. Russell, *J. Paleontol.* **39**, 497 (1965).
2. A. J. de Ricqlès, *Evol. Theory* **1**, 51 (1974).
3. R. T. Bakker, *Nature* **238**, 81 (1972).
4. R. T. Bakker, in *A Cold Look at the Warm-Blooded Dinosaurs,* R. D. K. Thomas, E. C. Olson, Eds. (Westview, Boulder, 1980), pp. 351–462.
5. J. O. Farlow, in *The Dinosauria,* D. B. Weishampel, P. Dodson, H. Osmólska, Eds. (Univ. California Press, Berkeley, 1990), pp. 43–55.
6. M. P. O'Conner, P. Dodson, *Paleobiology* **25**, 341 (1999).
7. F. Seebacher, G. C. Grigg, L. A. Beard, *J. Exp. Biol.* **202**, 77 (1999).
8. F. Seebacher, *Paleobiology* **29**, 105 (2003).
9. J. F. Gillooly, A. P. Allen, E. L. Charnov, *PLoS Biol.* **4**, e248 (2006).
10. H. Pontzer, V. Allen, J. R. Hutchinson, *PLoS ONE* **4**, e7783 (2009).
11. G. M. Erickson, *Trends Ecol. Evol.* **20**, 677 (2005).
12. J. Ruben, A. Leitsch, W. Hillenius, N. Geist, T. Jones, in *The Complete Dinosaur,* J. O. Farlow, M. K. Brett-Surman, Eds. (Indiana Univ. Press, Bloomington, 1997), pp. 505–518.
13. R. E. Barrick, W. J. Showers, *Science* **265**, 222 (1994).
14. H. C. Fricke, R. R. Rogers, *Geology* **28**, 799 (2000).
15. R. Amiot *et al.*, *Earth Planet. Sci. Lett.* **246**, 41 (2006).
16. K. Padian, J. R. Horner, in *The Dinosauria,* D. B. Weishampel, P. Dodson, H. Osmólska, Eds. (Univ. California Press, Berkeley, 2004), pp. 660–671.
17. A. Chinsamy, W. J. Hillenius, in *The Dinosauria,* D. B. Weishampel, P. Dodson, H. Osmólska, Eds. (Univ. California Press., Berkeley, 2004), pp. 643–659.
18. P. M. Sander *et al.*, *Biol. Rev. Camb. Philos. Soc.* **86**, 117 (2011).
19. T. J. Case, *Q. Rev. Biol.* **53**, 243 (1978).
20. A. J. de Ricqlès, in *A Cold Look at the Warm-Blooded Dinosaurs,* R. D. K. Thomas, E. C. Olson, Eds. (Westview, Boulder, 1980), pp. 103–139.
21. P. M. Sander, *Paleobiology* **26**, 466 (2000).
22. N. Klein, P. M. Sander, *Paleobiology* **34**, 247 (2008).
23. A. E. Dunham, K. L. Overall, W. P. Porter, C. A. Forster, in *Paleobiology of the Dinosaurs, GSA Special Paper 238,* J. O. Farlow, Ed. (Geological Society of America, Boulder, 1989), pp. 1–21.
24. J. R. Spotila, M. P. O'Conner, P. Dodson, F. V. Paladino, *Mod. Geol.* **16**, 203 (1991).
25. R. M. Alexander, *Palaeontology* **41**, 1231 (1998).
26. F. V. Paladino, M. P. O'Conner, J. R. Spotila, *Nature* **344**, 858 (1989).
27. Materials and methods are available as supporting material on *Science* Online.
28. P. Ghosh *et al.*, *Geochim. Cosmochim. Acta* **70**, 1439 (2006).
29. R. A. Eagle *et al.*, *Proc. Natl. Acad. Sci. U.S.A.* **107**, 10377 (2010).
30. F. Seebacher, R. M. Elsey, P. L. Trosclair 3rd, *Physiol. Biochem. Zool.* **76**, 348 (2003).
31. K. J. Dennis, D. P. Schrag, *Geochim. Cosmochim. Acta* **74**, 4110 (2010).
32. M. J. Kohn, T. E. Cerling, in *Reviews in Mineralogy and Geochemistry. Phosphates: Geochemical, Geobiological, and Materials Importance*, vol. 48, M. J. Kohn, J. Rakovan, J. M. Hughes, Eds. (Mineralogical Society of America and Geochemical Society, Washington, DC, 2002), pp. 455–488.
33. H. C. Fricke, R. R. Rogers, R. Backlund, C. N. Dwyer, S. Echt, *Palaeogeogr. Palaeoclimatol. Palaeoecol.* **266**, 13 (2008).
34. A. Clarke, P. Rothery, *Funct. Ecol.* **22**, 58 (2008).
35. M. J. Wedel, *Paleobiology* **29**, 243 (2003).
36. P. M. Sander, M. Clauss, *Science* **322**, 200 (2008).
37. E. H. Colbert, *Am. J. Sci.* **293**, (A), 1 (1993).

Acknowledgments: R.A.E. and J.M.E. are funded by National Science Foundation grant EAR-1024929. T.T. is funded by Deutsche Forschungsgemeinschaft (DFG) grants TU 148/2-1 and TU 148/4-1. A.K.T. is supported by the Division of Physical Sciences at UCLA and National Science Foundation grant EAR-0949191. We thank the Utah Museum of Natural History, the Oklahoma Museum of Natural History, the Berlin Museum für Naturkunde, the Aathal Dinosaurier Museum, D. Chure at Dinosaur National Monument, and the Wyoming Dinosaur International Society for the provision of specimens for analysis. We thank D. Schwarz-Wings for specimen identification and D. Goodreau for curatorial assistance. We also thank the stable isotope laboratories at Tübingen and Lyon for conducting phosphate $\delta^{18}O$ measurements. Lastly, thanks to J. Gillooly for provision of published data. This is contribution number 113 of the DFG Research Unit 533 "Biology of the Sauropod Dinosaurs: The Evolution of Gigantism." R.A.E. designed the project and experiments, performed the experiments, analyzed the data, and wrote the manuscript. J.M.E. and A.K.T. assisted with experimental design and data interpretation. Clumped isotope analyses were conducted in the lab of J.M.E. T.T. provided samples for the study, conducted phosphate oxygen isotope analysis, and assisted with data interpretation. T.S.M. assisted with isotope measurements and petrographic analyses. H.C.F., M.C., and R.L.C. provided samples for analysis and insights into the provenance of samples and data interpretation.

Supporting Online Material

www.sciencemag.org/cgi/content/full/science.1206196/DC1
Materials and Methods
SOM Text
Figs. S1 to S6
Tables S1 to S10
References (*38*–*103*)

28 March 2011; accepted 3 June 2011
Published online 23 June 2011;
10.1126/science.1206196

A Common Scaling Rule for Abundance, Energetics, and Production of Parasitic and Free-Living Species

Ryan F. Hechinger,[1]* Kevin D. Lafferty,[1,2] Andy P. Dobson,[3,4] James H. Brown,[5] Armand M. Kuris[1]

The metabolic theory of ecology uses the scaling of metabolism with body size and temperature to explain the causes and consequences of species abundance. However, the theory and its empirical tests have never simultaneously examined parasites alongside free-living species. This is unfortunate because parasites represent at least half of species diversity. We show that metabolic scaling theory could not account for the abundance of parasitic or free-living species in three estuarine food webs until accounting for trophic dynamics. Analyses then revealed that the abundance of all species uniformly scaled with body mass to the −¾ power. This result indicates "production equivalence," where biomass production within trophic levels is invariant of body size across all species and functional groups: invertebrate or vertebrate, ectothermic or endothermic, and free-living or parasitic.

General ecological theory should apply to all species, and thus should include the parasites that represent at least half of species diversity (*1*–*3*). A goal of the metabolic theory of ecology is to broadly explain and predict local species abundance by considering how metabolic rate scales with body size and temperature (*4*, *5*). Although studies have documented the scaling of parasite abundance with body size within individual hosts (*6*, *7*), none have examined the scaling of parasites alongside co-occurring free-living species. This omission is potentially critical because, in addition to their great diversity, there are other factors indicating that the inclusion of parasites can test and refine general rules for abundance and body-size scaling.

Parasites differ from free-living consumers in ways that can violate assumptions made by current models of abundance and diversity. For instance, because parasites are smaller than their hosts, they invert consumer-resource body-size ratios, which are often assumed to be constant and larger than 1 (*4*, *8*–*10*). Further, parasites might be rarer than other small consumers, as they tend to occupy higher trophic levels to which the flow of resources is constrained by trophic

[1]Marine Science Institute and Department of Ecology, Evolution, and Marine Biology, University of California, Santa Barbara, CA 93106, USA. [2]Western Ecological Research Center, U.S. Geological Survey, Marine Science Institute, University of California, Santa Barbara, CA 93106, USA. [3]Department of Ecology and Evolutionary Biology, Princeton University, Princeton, NJ 08544, USA. [4]Santa Fe Institute, Santa Fe, NM 87501, USA. [5]Department of Biology, University of New Mexico, Albuquerque, NM 87131, USA.

*To whom correspondence should be addressed. E-mail: hechinger@lifesci.ucsb.edu

transfer efficiency (the fraction of energy in resource populations that is converted into consumer populations) (*11*–*13*). On the other hand, parasites appear to grow and reproduce at higher rates than their free-living relatives (*14*), potentially reflecting higher assimilation and production efficiencies, which are major components of trophic transfer efficiency (*11*–*13*). These differences highlight the importance of simultaneously considering parasites and free-living species to develop empirical generalizations and theory concerning species abundance, body-size scaling, and trophic dynamics.

Among species, abundance typically decreases with increasing body size because larger individuals require more resources. Resource requirements parallel whole-organism metabolic rates, which increase with body size as M^{α}, where M is body mass and α is a scaling exponent with a positive sign. Consequently, when differently sized species have, on average, equal access to resources, population abundance N is predicted to scale as

$$N = iM^{-\alpha} \quad (1)$$

where i is a normalization constant (*4*, *5*, *15*). Body temperature also influences abundance, because metabolic rates can increase over a broad temperature range (*5*, *16*). All else being equal, abundance decreases with increasing temperature because each individual requires more resources (*4*). We can add temperature dependence, so that

$$N = iM^{-\alpha}D^{-1} \quad (2)$$

where D represents a dimensionless temperature-dependence term (*17*, *18*). This can be captured by an Arrhenius equation formulation that expresses exponential temperature effects relative to a standard: $\exp[(E/k)(T - T_o)/TT_o]$, where E is the activation energy, k is the Boltzmann constant, T is the body temperature, and T_o is the standard temperature (*11*, *16*). We can rearrange Eq. 2 to provide an estimate of "temperature-corrected" abundance (*4*, *17*): $N_{temp} = ND = iM^{-\alpha}$. Abundance–body size relationships are usually analyzed by linear regression after logarithmic transformation, so that $\log N_{temp} = \log i - \alpha \log M$, and the slope gives the exponent α. Because whole-organism metabolic rates across a broad range of multicellular organisms scale, on average, as $M^{3/4}$ (*5*, *16*, *19*, *20*), their abundance is predicted to scale, on average, as $M^{-3/4}$ (*4*, *8*–*10*, *21*, *22*).

Few studies (*23*, *24*) have quantified the scaling of local abundance for diverse groups of species that coexist in an ecosystem and span a wide range of body sizes and basic physiologies, and none have included parasites. Recent investigations of three estuarine food webs in California and Baja California provide data that permit such an analysis (*25*, *26*) (table S1). In all three estuaries, species abundance decreased by 11 orders of magnitude as body size increased by 11 orders of magnitude (Fig. 1, A to C). A single regression did not adequately describe the relationship, primarily because slopes for parasites (–0.50 to –0.63) were consistently shallower than the slopes characterizing free-living species (–1.26 to –1.36) (Fig. 1, A to C). Furthermore, parasites were consistently less abundant than free-living species of similar body size. Despite being two to three orders of magnitude smaller than the average free-living invertebrate species, the average parasite species was at least one order of magnitude less abundant. As expected, using N_{temp} to factor in the higher body temperature of birds relative to the other animals [characterized by ambient environmental temperatures (*11*)] provided very similar relationships (Fig. 1, D to F). Thus, in these analyses, the scaling of abundance with body size does not support a common scaling exponent, –¾ or otherwise, for parasitic and free-living species.

However, the above analysis does not account for the flow of energy among trophic levels. Inefficiencies in exploitation, assimilation, and production ensure that trophic transfer efficiency is less than 100% (*12*, *13*). Thus, fewer resources are available to higher trophic levels. Previous studies have added trophic transfer efficiency to scaling relationships by modifying the scaling exponent, assuming a particular transfer efficiency and that consumer-resource body-size ratios are fixed and larger than 1 (*4*, *8*–*10*, *21*, *27*, *28*). Free-living assemblages will sometimes violate this assumption, potentially explaining why adding trophic transfer efficiency in this manner performed no better than ignoring it did in a previous analysis of 121 food webs (*29*). Moreover, simultaneous consideration of parasitic and free-living species will always strongly violate assumptions of consistent consumer-resource body-size ratios or of a positive relationship between trophic level and body size.

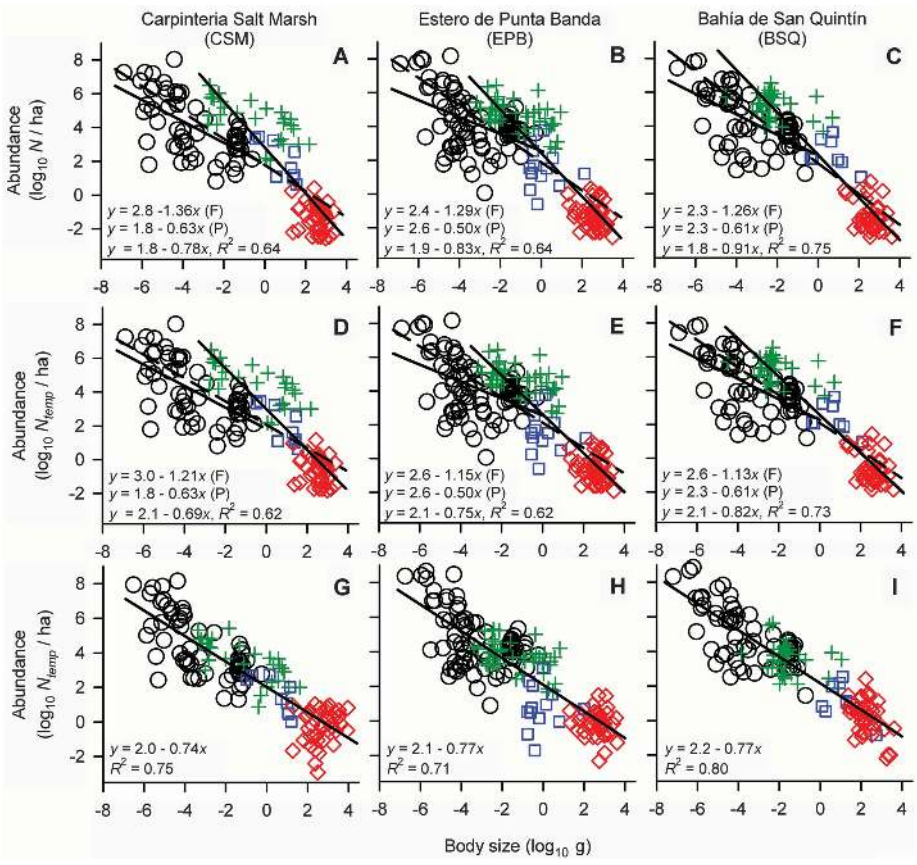

Fig. 1. Abundance as a function of body size for parasitic and free-living species in three estuaries: Carpinteria Salt Marsh (CSM), Estero de Punta Banda (EPB), and Bahía de San Quintin (BSQ). (**A** to **C**) Abundance versus body size reveals that a single regression line cannot adequately fit the data (general linear models: all interaction Ps < 0.0001; tables S2 and S3). Solid lines and top two equations give the slopes and intercepts for parasitic (P) and free-living (F) species; slope 95% confidence limits: CSM, ±0.14; EPB, ±0.13; BSQ, ±0.11. The broken lines, bottom equations, and R^2s pertain to pooled data. (**D** to **F**) Temperature-corrected abundance versus body size gives relationships very similar to those seen in (A) to (C), although bird abundance is shifted up by about half an order of magnitude, leading to slightly shallower slopes for free-living and pooled data. Lines and equations as in (A) to (C); slope 95% confidence limits: CSM, ±0.13; EPB, ±0.12; BSQ, ±0.10. (**G** to **I**) Temperature-corrected abundance versus body size, statistically controlling for trophic level (Fig. 3 and tables S4 and S5). The scaling slopes are all consistent with the –¾ predicted by metabolic scaling, as slightly modified for the distribution of the number of species along the body-size axis (*11*); slope 95% confidence limits: CSM, ±0.073; EPB, ±0.073; BSQ, ±0.063. The R^2 values represent partial R^2s for body size. Symbol key for all figures: circles, parasites; crosses, invertebrates; squares, fish; diamonds, birds.

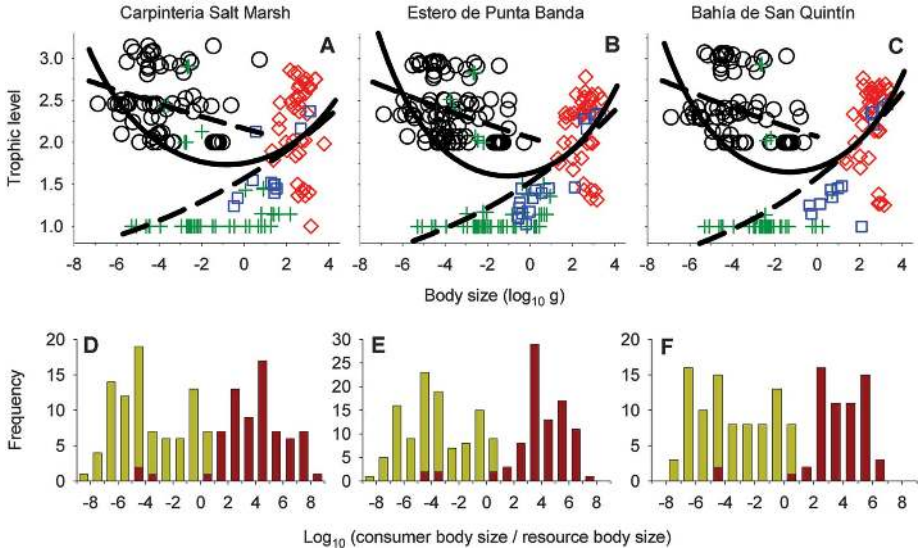

Fig. 2. Variation in trophic level with body size, and in consumer-resource body-size ratios, for parasitic and free-living species in three estuarine food webs. (**A** to **C**) Relationship between trophic level and body size. Dashed lines represent separate relationships for parasitic and free-living species (Poisson regressions, all interaction *P*s < 0.0001; tables S6 and S7), and solid lines represent significant curvilinear relationships for the two groups pooled (Poisson regressions, all quadratic term *P*s < 0.0001; tables S8 and S9). Symbols as in Fig. 1. (**D** to **F**) Frequency distributions of logged consumer-resource body-size ratios. Shaded portions of the histograms represent parasites and unshaded portions represent free-living consumers. Values less than 0 are for consumers that are smaller than their resources. These data show wide variation in consumer-resource body-size ratios, in contrast to the more constrained values observed when ignoring parasites.

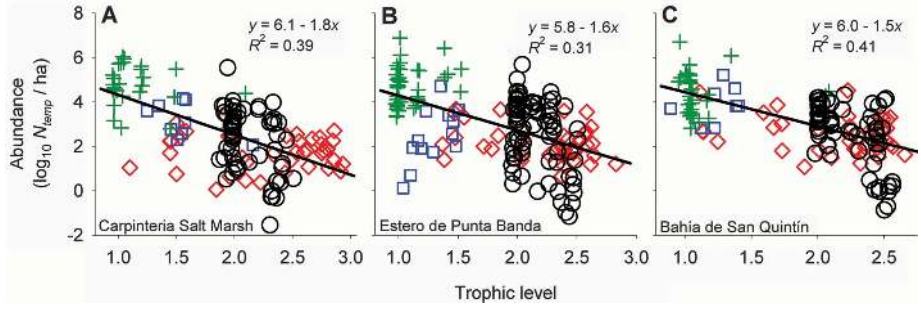

Fig. 3. (**A** to **C**) Abundance as a function of trophic level for parasitic and free-living species in three estuaries. Temperature-corrected abundance decreases with trophic level, as revealed by statistically controlling for body size (Fig. 1, G to I, and tables S4 and S5). The anti-log of the slope provides an estimate of ε, the overall trophic transfer efficiency in each ecosystem. Symbols as in Fig. 1.

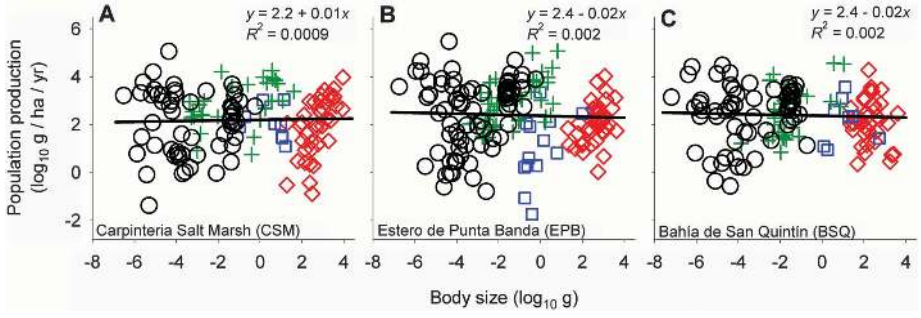

Fig. 4. (**A** to **C**) Population biomass production versus body size for parasitic and free-living species in three estuaries, statistically controlling for trophic level. The slopes of the fitted lines in each estuary are indistinguishable from zero (tables S10 and S11); 95% confidence limits: CSM, ±0.073; EPB, ±0.073; BSQ, ±0.063. Symbols as in Fig. 1.

Indeed, in the estuaries studied here, the relationship between trophic level and body size is U-shaped when parasites are included (Fig. 2, A to C) (*11*). Further, including parasites approximately doubled the range of observed consumer-resource body-size ratios because parasites, in contrast to typical free-living consumers, are much smaller than their resources (Fig. 2, D and E). This highlights the need to incorporate trophic transfer efficiency independent of body size, or of any assumed body-size associations, to derive broadly applicable and realistic scaling relationships. Although rarely done [e.g., (*4*, *27*, *28*)], we can use a separate, multiplicative term to capture the loss of energy among trophic levels. We can modify Eq. 2 to incorporate the exponential decrease of abundance with increasing trophic level (L) as

$$N_{\text{temp}} = iM^{-\alpha}\varepsilon^{L} \quad (3)$$

where ε is trophic transfer efficiency (a proportion) and basal trophic level = 0 (*11*). Linearizing Eq. 3 by log transformation gives

$$\log N_{\text{temp}} = \log i - \alpha \log M + \log \varepsilon \cdot L \quad (4)$$

Equation 4 can be analyzed directly with a general linear model that incorporates L and log M as predictor variables and provides empirical estimates of the scaling exponent and trophic transfer efficiency. After controlling for body size, as predicted, abundance decreased with increasing trophic level (Fig. 3, A to C). The estimates of average transfer efficiency across all species were $\varepsilon \approx 0.025$, toward the low end of the range typically reported (*12*, *13*, *30*). These estimates of ecosystem-wide transfer efficiency may be accurate, but they may also be a consequence of the theoretical assumption that only the bottom-up process of resource supply constrains abundance. The effect of trophic level may also include top-down effects of consumers (predators or parasites) on resource (prey or host) abundance, which can be explored by future research.

The use of Eq. 4 to incorporate trophic dynamics revealed a uniform ecosystem-wide scaling of abundance with body size in all three estuaries (Fig. 1, G to I). The relationships no longer differed between parasites and free-living species (table S4). Further, the slopes of the uniform abundance versus body-size relationships were all very close to –¾, as predicted by a ¾ scaling of metabolic rate with body size. Hence, after accounting for temperature, trophic level, and trophic transfer efficiency, a single line consistently explained abundance as a function of body size across diverse taxonomic and functional groups.

For physiologically similar multicellular organisms, a –¾ scaling of abundance with body size implies the average "energetic equivalence" of differently sized species because a single line describes the average $M^{3/4}$ scaling of whole-organism metabolic rates (*4*, *15*, *22*, *31*, *32*). In these cases, the population energy flux F (the product of individual metabolic rate and population abundance) scales invariant of body size, as $M^{3/4}M^{-3/4} = M^{0}$ (fig. S1). However, a single line

does not adequately describe the $M^{3/4}$ scaling of whole-organism metabolism for the species in our study because they span different physiological groups with different normalization constants (*4*, *16*) (fig. S1). Hence, the uniform abundance scaling documented here across all species indicates that, at any particular trophic level, populations of similarly sized species in different physiological groups flux different amounts of energy: endotherms > vertebrate ectotherms > parasitic or free-living invertebrates (fig. S1).

The uniform scaling of abundance found here has another general implication—that of "production equivalence." Specifically, species at the same trophic level produce biomass at the same average rate across all body sizes and functional groups. This occurs because, in contrast to metabolic rates, a single line can describe the $M^{3/4}$ scaling of individual biomass production, P_{ind}, for organisms of different physiological groups (*31*) (fig. S1). Consequently, the population production rate equals $P_{pop} = P_{ind}N$, which scales as $M^{3/4}M^{-3/4} = M^{0}$. Indeed, estimating population production for the species in the three estuaries supports the existence of this invariant biomass production with body size (Fig. 4 and fig. S1) (*11*). Thus, although population energy flux (and, consequently, demand on resources) may vary among physiological groups, opposing differences in production efficiency among these groups cause population biomass production to scale invariant of body size across all groups. Because production reflects biomass availability to consumers, production equivalence indicates a comparable ecological relevance for any single species within a trophic level, regardless of body size or functional group affiliation: invertebrate or vertebrate, ectotherm or endotherm, free-living or parasitic.

Accommodating parasitic and free-living species into a common framework highlights the utility of Eq. 3 to incorporate body size, temperature, and food-web information into ecological scaling theory in a simple and generally applicable way. Equations 3 and 4 may allow testing of the generality of the findings documented here for any ecosystem and any form of life.

References and Notes

1. P. W. Price, *Evolutionary Biology of Parasites* (Princeton Univ. Press, Princeton, NJ, 1980).
2. T. de Meeûs, F. Renaud, *Trends Parasitol.* **18**, 247 (2002).
3. A. P. Dobson, K. D. Lafferty, A. M. Kuris, R. F. Hechinger, W. Jetz, *Proc. Natl. Acad. Sci. U.S.A.* **105** (suppl. 1), 11482 (2008).
4. J. H. Brown, J. F. Gillooly, A. P. Allen, V. M. Savage, G. B. West, *Ecology* **85**, 1771 (2004).
5. R. H. Peters, *The Ecological Implications of Body Size* (Cambridge Univ. Press, Cambridge, 1983).
6. P. Arneberg, A. Skorping, A. F. Read, *Am. Nat.* **151**, 497 (1998).
7. S. Morand, R. Poulin, *Evol. Ecol. Res.* **4**, 951 (2002).
8. J. H. Brown, J. F. Gillooly, *Proc. Natl. Acad. Sci. U.S.A.* **100**, 1467 (2003).
9. S. Jennings, S. Mackinson, *Ecol. Lett.* **6**, 971 (2003).
10. D. C. Reuman, C. Mulder, D. Raffaelli, J. E. Cohen, *Ecol. Lett.* **11**, 1216 (2008).
11. See supporting material on *Science* Online.
12. R. L. Lindeman, *Ecology* **23**, 399 (1942).
13. D. G. Kozlovsky, *Ecology* **49**, 48 (1968).
14. P. Calow, *Parasitology* **86**, 197 (1983).
15. J. Damuth, *Nature* **290**, 699 (1981).
16. J. F. Gillooly, J. H. Brown, G. B. West, V. M. Savage, E. L. Charnov, *Science* **293**, 2248 (2001).
17. A. P. Allen, J. H. Brown, J. F. Gillooly, *Science* **297**, 1545 (2002).
18. W. R. Robinson, R. H. Peters, J. Zimmermann, *Can. J. Zool.* **61**, 281 (1983).
19. M. Kleiber, *Hilgardia* **6**, 315 (1932).
20. A. M. Hemmingsen, *Repts. Steno. Hosp. Copenhagen* **9**, 7 (1960).
21. H. Cyr, in *Scaling in Biology*, J. H. Brown, G. B. West, Eds. (Oxford Univ. Press, Oxford, 2000), pp. 267–295.
22. J. Damuth, *Biol. J. Linn. Soc. London* **31**, 193 (1987).
23. H. Cyr, J. A. Downing, R. H. Peters, *Oikos* **79**, 333 (1997).
24. J. E. Cohen, T. Jonsson, S. R. Carpenter, *Proc. Natl. Acad. Sci. U.S.A.* **100**, 1781 (2003).
25. R. F. Hechinger *et al.*, *Ecology* **92**, 791 (2011).
26. A. M. Kuris *et al.*, *Nature* **454**, 515 (2008).
27. T. D. Meehan, *Ecology* **87**, 1650 (2006).
28. B. J. McGill, *Am. Nat.* **172**, 88 (2008).
29. D. C. Reuman *et al.*, *Adv. Ecol. Res.* **41**, 1 (2009).
30. D. Baird, J. M. Mcglade, R. E. Ulanowicz, *Philos. Trans. R. Soc. B* **333**, 15 (1991).
31. S. K. M. Ernest *et al.*, *Ecol. Lett.* **6**, 990 (2003).
32. S. Nee, A. F. Read, J. J. D. Greenwood, P. H. Harvey, *Nature* **351**, 312 (1991).

Acknowledgments: We thank S. Sokolow, J. McLaughlin, J. Childress, and J. Damuth for discussion or comments on the manuscript. Supported by NSF/NIH EID grant DEB-0224565 and by CA Sea Grant R/OPCENV-01. The analyses in this manuscript used data published in Hechinger *et al.* (*25*), available at Ecological Archives (accession no. E092-066).

Supporting Online Material

www.sciencemag.org/cgi/content/full/333/6041/445/DC1
Materials and Methods
Figs. S1 and S2
Tables S1 to S11
References (*33*–*48*)

15 February 2011; accepted 27 May 2011
10.1126/science.1204337

Terraces in Phylogenetic Tree Space

Michael J. Sanderson,[1]* Michelle M. McMahon,[2] Mike Steel[3]

A key step in assembling the tree of life is the construction of species-rich phylogenies from multilocus—but often incomplete—sequence data sets. We describe previously unknown structure in the landscape of solutions to the tree reconstruction problem, comprising sometimes vast "terraces" of trees with identical quality, arranged on islands of phylogenetically similar trees. Phylogenetic ambiguity within a terrace can be characterized efficiently and then ameliorated by new algorithms for obtaining a terrace's maximum-agreement subtree or by identifying the smallest set of new targets for additional sequencing. Algorithms to find optimal trees or estimate Bayesian posterior tree distributions may need to navigate strategically in the neighborhood of large terraces in tree space.

Phylogenetic tree space, the collection of all possible trees for a set of taxa, grows exponentially with the number of taxa, creating computational challenges for phylogenetic inference (*1*). Nonetheless, phylogenetic trees and comparative analyses based on them are growing larger, with several exceeding 1000 species [e.g., (*2*)] and a recent one exceeding 50,000 (*3*). Understanding the landscape of tree space is important because heuristic algorithms for inferring trees using maximum likelihood (ML), maximum parsimony (MP), and Bayesian inference navigate through parts of this space guided by notions of its structure [e.g., (*4*)]. Moreover, analyses that use phylogenies to study evolutionary processes typically sample from tree space to obtain a good statistical "prior" distribution of phylogenetic relationships used in subsequent comparative analyses, but the design of sampling strategies hinges on the structure of tree space (*5*).

An important advance in understanding tree space was the formulation of the concept of "islands" of trees with similar MP or ML optimality scores (*6*, *7*). Trees belong to the same island if they are near each other in tree space and have optimality scores of L or better with respect to some data matrix. Distance in tree space can be measured by the number of rearrangements required to convert one tree to another. Nearest neighbor interchanges (NNIs), for example, are rearrangements obtained by swapping two subtrees around an internal branch of a tree. Conflicting signals or missing data can result in multiple large tree islands, separated by "seas" of lower-scoring trees, a landscape that can only be characterized by lengthy searches through tree space [e.g., (*8*)]. Empirical studies of phylogenetic tree islands flourished in the context of the single-locus data sets that were common in the 1990s. However, maintaining the same level of accuracy in the larger trees studied today requires combining multiple loci (*9*). The most widely used protocol for data combination is concatenation of multiple alignments of orthologous sequences, one next to another, analyzed as one "supermatrix," a procedure justified when gene tree discordance is low between loci (*10*). Notably, a hallmark of almost all large supermatrix studies is a sizable proportion of missing entries.

[1]Department of Ecology and Evolutionary Biology, University of Arizona, Tucson, AZ 85721, USA. [2]School of Plant Sciences, University of Arizona, Tucson, AZ 85721, USA. [3]Allan Wilson Centre for Molecular Ecology and Evolution, University of Canterbury, Christchurch, New Zealand.

*To whom correspondence should be addressed. E-mail: sanderm@email.arizona.edu

www.sciencemag.org/cgi/content/full/333/6041/445/DC1

Supporting Online Material for

A Common Scaling Rule for Abundance, Energetics, and Production of Parasitic and Free-Living Species

Ryan F. Hechinger,* Kevin D. Lafferty, Andy P. Dobson, James H. Brown, Armand M. Kuris

*To whom correspondence should be addressed. E-mail: hechinger@lifesci.ucsb.edu

Published 22 July 2011, *Science* **333**, 445 (2011)
DOI: 10.1126/science.1204337

This PDF file includes:

Supporting Online Material (SOM)

Materials and Methods

Study systems.

The three estuaries are tidal wetlands in California and Baja California: Carpinteria Salt Marsh (CSM), Estero de Punta Banda (EPB), and Bahía Falsa in Bahía San Quintín (BSQ). The total areas were 61 ha for CSM, 707 ha for EPB, and 144 ha for BSQ (these areas exclude subtidal lagoon portions of BSQ and EPB).

Species abundance and body-size data.

Data for abundance versus body-size analyses come from quantitative, stratified random sampling of the three estuaries as detailed in Kuris et al. (*26*). Hechinger et al. (*25*) present the species and stage-specific abundance and body-size information for each estuary. The bird assemblage primarily uses the estuaries in the fall and winter seasons, and we use the higher quality winter abundance data.

Body-sizes were estimated as described in Kuris et al. (*26*). For most free-living species, body size represents estimates of the average body mass for individuals of each species as they occurred in the random sampling. Body mass was wet-weight including hard parts. For birds, we used published records of average weight (*33, 34*). The body size of most parasites came from either directly weighing individuals or by estimating their mass by multiplying biovolume estimates by a tissue density of 1.1 g/mL (*5*). Because parasitic castrators of crustaceans grow in close proportion to host growth (e.g., $r = 0.84$), we estimated parasite to host weight ratios for these groups and then multiplied this ratio by the mass of infected hosts. The body sizes of trematode parthenitae represent the aggregate mass of parthenitae in a single infection, as described by Hechinger et al. (*35*).

Although many of the animals in our system grow indeterminately, average body size (per life-cycle stage) is a good measure of body size because any intraspecific variation in body size variation is small compared to the greater than 10 orders of magnitude variation among species.

Many of the quantified parasites have complex life cycles, with distinct stages having very different body sizes, morphologies, and strategies of resource use. Species abundance for a particular species was therefore sometimes separately quantified at more than one life stage (Table S1). In our main analyses, we treated such stages separately. As discussed below, this did not influence our findings.

Trophic level.

Hechinger et al. (*25*) present food webs for these three estuaries. The species composition of the food webs includes all the species in the present abundance versus body size analyses (i.e., those from the systematic quantitative sampling presented in Kuris et al. (*26*)). The published food webs also include species that were not encountered in Kuris et al. (*26*). Because Hechinger et al. (*25*) provide body-size estimates for many of these additional species, we were able to include many of these species in the assessments of trophic level with body size, and in our assessments of consumer-resource body size ratios. The published food webs also allowed us to separately treat different life stages for parasitic and free-living species that have complex life cycles where different stages have very distinct body sizes and trophic relationships.

We note that the small free-living invertebrates at high trophic levels in Fig. 2 are "raptorial predators" (e.g., a nemertean and a wolf spider) and "micropredators" (e.g., a fish louse, adult mosquitoes, a pyramidellid mollusc).

Given that many species in these webs feed on prey at various trophic levels, trophic level is correctly expressed fractionally, being 1 plus the average trophic level of a consumer's resources. We used "short-weighted" trophic level, which provides a more realistic estimate of the trophic level by giving greater weight to resources at lower trophic levels (and thus more likely to be encountered, Williams and Martinez' (*36*)). To compute these values, we used the software, Network3D (written by R.J. Williams and provided by the Pacific Ecoinformatics and Computational Ecology Lab, www.foodwebs.org (*37, 38*)). For simplicity, we defined basal trophic levels as $L = 0$. If desirable to set basal trophic levels to $L = 1$, the exponent in Eq. 3 should simply be changed from L to $L - 1$.

Consumer-resource body-size ratios.
We first calculated a consumer-resource body-size ratio for every trophic link in the webs using the mean body sizes for each species life stage (node) reported for each estuary (*25*). Then, for each consumer, we averaged the consumer-resource body-size ratio among the consumer's links. As mentioned above, we were able to calculate consumer-resource body-size ratios for some food web species whose abundances were not captured by our quantitative abundance sampling, but for which we did have body size information (see Table S1 and Hechinger et al. (*25*)).

We note that, in Fig. 2, the log consumer-resource body-size ratio is slightly larger than 0 for eight parasitic castrator trematode species, because these parasites grow to be ~10-40% the mass of their snail hosts (*35*), tend to infect larger hosts, and consequently can have a slightly larger average size than the average host.

Temperature and temperature effects.
The formulation of the Arrhenius equation that we used for D, $e^{(E/k)((T-To)/TTo)}$, allowed us to express temperature effects relative to the ambient temperature within each estuary. In this study, all animals except for birds are ectothermic, and we assumed that their body temperatures were characterized, on average, by each estuary's ambient temperature (we did not include parasites of birds in the abundance analyses). Hence, as T_o, we used the ambient water temperature characterizing the estuaries during summer-fall months: 19°C for CSM, 21.6 °C for EPB, and 20.0 °C for BSQ (*39-41*). We assigned a body temperature of 40 °C to the endothermic birds. Temperature was expressed in °K. This formulation of the Arrhenius equation scales 1:1 with the term, $e^{-E/kT}$, that is commonly used in ecological scaling research (e.g., see *4, 17, 27, 31*). We used it because it allowed temperature-correction of abundance to maintain intuitively sensible units. Because we performed analyses for each estuary separately, the temperature-corrected abundance, $N_{temp} = N \cdot D$, adjusted the abundance of the endothermic birds and did not modify (multiplied by 1) the abundance of the other (ectothermic) animals. We used N_{temp} instead of leaving D^{-1} as a predictor variable primarily to preclude problems associated with collinearity in our datasets between temperature and body size; temperature differences were limited to large endotherms (birds) versus all other, smaller animals. We used 0.63 eV for the average activation energy, E, and 8.62×10^{-5} eV·K^{-1} for Boltzmann's constant, k (*4, 16*).

Theoretical incorporation of trophic transfer efficiency.
Trophic transfer efficiency (the fractional transfer of production or energy up trophic levels) is a composite of several sequential efficiencies (*12, 13, 42, 43*). A useful way to express these efficiencies is: (1) exploitation or consumption efficiency (the proportion of a lower trophic level's production that is removed or ingested), (2) assimilation efficiency (the proportion of ingested material that is converted into usable energy), and (3) production efficiency (or "tissue growth efficiency", the proportion of assimilated energy that is converted into new biomass via growth or reproduction). When the physiological type of organism varies with trophic level (e.g., vertebrates tending to be at higher trophic level), the *component* efficiencies greatly vary among trophic level, often in contrasting directions (*12, 13*). For instance, for free-living animals, production efficiency can decrease with increasing trophic level, given greater maintenance costs and heat loss. However, exploitation efficiency can simultaneously increase, which is intuitive to the extent the greater respiration reflects greater foraging rates. Contrasting relationships of the component ecological efficiencies result in greater consistency among trophic levels concerning the *overall* trophic transfer efficiency. This phenomenon was described by Lindeman (*12*) (perhaps unclearly) and clarified by Kozlovsky (*13*).

Brown et al. (*4*) transiently incorporated trophic transfer efficiency into metabolic scaling theory the way Eq. 3 does (using ε^L). A similar effort to ours at incorporating trophic transfer efficiency into metabolic-scaling abundance theory was made by Meehan (*27*). Following Gillooly et al's (*44*) model depicting the transfer of energy up a single trophic step, Meehan's theoretical approach included two transfer efficiency terms: (1) a term for the proportion of primary production assimilated by the next trophic level (Meehan's a, which in the breakdown above equates to exploitation efficiency times assimilation efficiency) and (2), a production efficiency term (Meehan's ε, equivalent to the above described production efficiency). To incorporate the loss of energy up trophic levels, Meehan's approach assumed that only production efficiency was involved in the trophic transfer efficiency term. Exploitation and assimilation efficiencies were only applied as a constant to the first transfer of energy from primary producers to primary consumers. However, as discussed above, all three component efficiencies (exploitation x assimilation x production) comprise trophic transfer efficiency and should propagate with trophic level, as they do in our incorporation of ε^L in Eq. 3. Interestingly, the details of the theory did not affect Meehan's empirical analysis, because in log-log space the theoretically constant exploitation x assimilation term was subsumed within the intercept. The production efficiency term estimated from the model was actually the overall transfer efficiency (exploitation x assimilation x production). Thus, when appropriately understood (and barring a problem in the use of log binning (*45*)), the analysis in Meehan (*27*) is important for demonstrating the utility of including trophic transfer efficiency in a simple, multiplicative way, as done by McGill (*28*) and as done here.

Abundance versus body-size analyses.
To assess the adequacy of the theoretical models for abundance represented by Eqs. 1-3 and the theory for population production, we used general linear models (GLMs) (*46, 47*) in JMP v. 8 on the logged version of the equations. Ordinary least squares and "model 1 regression" analyses are justified given the expectation that error in abundance estimates dwarfs error in the predictor variables, particularly body size. Model 1 analyses are further supported by the extensive

examination of alternative regression techniques of abundance and body size in 166 webs by Reuman et al. (*29*).

To examine whether parasites and free-living species scaled differently with body size, we included "free-living or parasitic" as an additional (categorical) variable in the GLMs, along with its interaction with log body size. *F*-tests allowed evaluation of whether these variables significantly improved the GLM.

We assessed GLM model adequacy using several types of residual plots (*46, 47*). Inspecting plots of residuals versus predicted values assured that models met assumptions concerning variance homogeneity and serial independence of the data. There was weak heterogeneity of variance caused by the bird abundance data. However, the large magnitude and high *P*-values of the effects in these analyses preclude concern about this. Normal quantile plots with Lillifors 95% confidence limit curves documented approximate normality of the residuals. Plotting residuals versus log M x L ensured the lack of a strong interaction between these main effects in the GLM based on Eq. 4 (*46*).

It is also worth noting the obvious fact that the data points within each estuary have some interdependencies. The species interact with one another in a diversity of consumer-resource relationships and the species are also not independent concerning phylogeny. Although there is debate about whether phylogenetic control is reasonable in abundance research, imposing phylogenetic control on data that spans a wide range of taxa will not alter conclusions (*48*). Further, some species are represented by two distinct life stages. However, the life stages differ in body size, morphology, and resource use, warranting their independent inclusion into these initial "bottom-up" analyses. However, including the separate life stages did not influence our findings, as assessed for the main abundance versus body-size analyses incorporating trophic level (depicted in Fig. 1G-I). Randomly excluding one life stage, from those species represented by two, yielded results with slopes and intercepts statistically indistinguishable from the analyses using separate life stages, with full-model R^2s within 0.01.

Finally, we note that the analyses presented here have focused on examining the performance of broad and generally applicable scaling theory and patterns. Future work can explore the finer details of scaling within the patterns documented in this manuscript (e.g., interactions among functional groups and trophic level and body size).

Adjusting for species body-size distributions.
The number of species sharing resources is an additional factor that can influence predictions of local species abundance versus body size (*10*). This is most easily understood in that a given amount of resources supports a certain amount of individuals, which are then partitioned into different species. Controlling for resources (trophic level), we predict that log animal species abundance will scale with log body size with an slope of -¾ if the number of species does not vary along the log body-size axis, or, equivalently, if the number of species isometrically decreases with unlogged body size (that is, with an exponent of -1). Examining the log of the number of species *normalized by linear bin-width* versus the mid-point of log body size-class bins provides an estimate of the latter exponent (*10, 45*); so does a non-linear regression fit to the cumulative density function (cdf) of species body sizes (*10, 45*). Adding 1 to the estimated

exponents and subtracting the value from -¾ provides the theoretically expected scaling of species abundance versus body size (*10*).

Regressions on the log of the normalized number of species versus log size class indicate that species mean body size distributions have a slight effect on the predicted scaling exponents of abundance versus body size (Fig. S2). Although the confidence limits for each slope overlap -1, this is expected given the low sample size. Fitting a truncated Pareto distribution (*45*) using non-linear regression gave almost identical estimates with 95% confidence limits that never overlapped -1. Because the residuals sometimes deviated from normality in the non-linear regressions, we use the almost identical (always within 0.01) estimates from the normalized log binning. Thus, the predicted scaling of abundance with body size is slightly adjusted downward from -0.75 by 0.04 (CSM), 0.03 (EPB), and 0.02 (BSQ).

Population production.
We estimated each species' population production as $P_{pop} = P_{ind}\, N_{temp}$. Individual biomass production, P_{ind}, was estimated using the empirically established temperature-corrected individual biomass production versus body size relationship from Ernest et al. (*31*). We used their formula for "all species" with the normalization constant of 10.3 and the theoretical exponent of 0.75 instead of 0.72, and converted kg to g. We also converted their temperature-correction to the standardized correction used in this manuscript. We used N_{temp} instead of N so that the temperature correction in P_{ind} would cancel out; temperature-correction shifts upward endotherm abundance as $N\,D$ and shifts downward endotherm individual production as $P_{ind}D^{-1}$.

SOM Figures and Tables

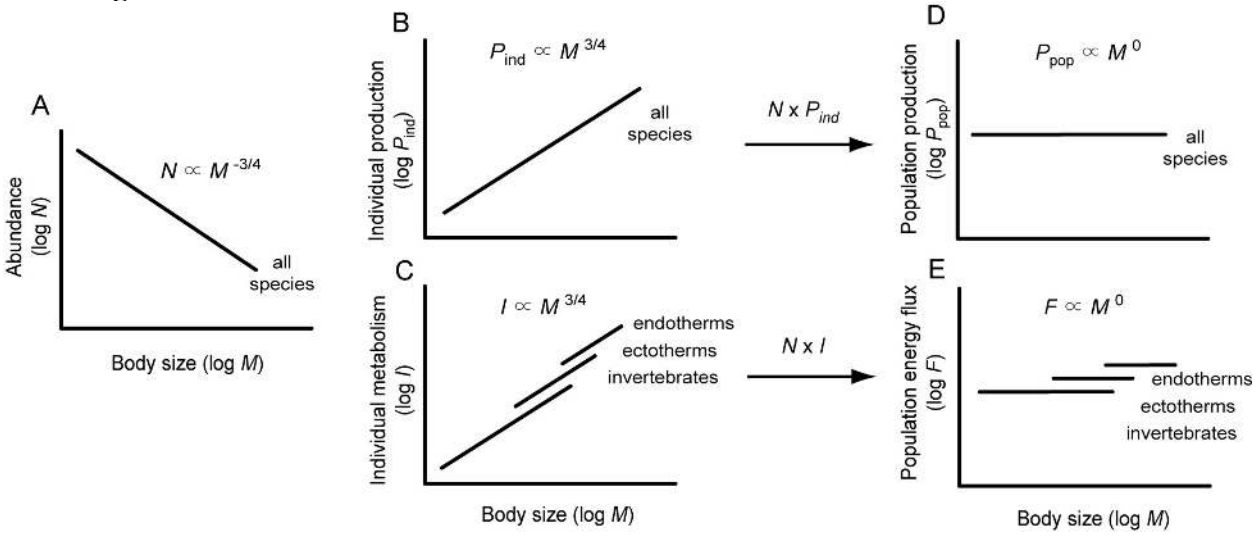

Fig. S1. A graphical model clarifying the body-size scaling of abundance, production, and energetic flux.
(A) The uniform $M^{-3/4}$ scaling of temperature-corrected abundance observed across all species holding trophic level constant, as documented in this manuscript. (B) The approximately uniform $M^{3/4}$scaling of individual biomass production documented in Ernest et al. (*31*) as occurring across a wide range of multicellular species. (C) The $M^{3/4}$scaling of individual whole-body metabolism (individual energy flux), showing the different normalization constants for different physiological groups as documented in Gillooly et al. (*16*). (D) The invariant scaling of population production ("production equivalence") observed across all species within a trophic level, as documented in this study (Fig. 4). Note that the temperature-correction terms in abundance and individual production cancel out so that temperature effects are not removed or hidden. (E) The lack of "energetic equivalence" indicated in our data that include species spanning different physiological groups.

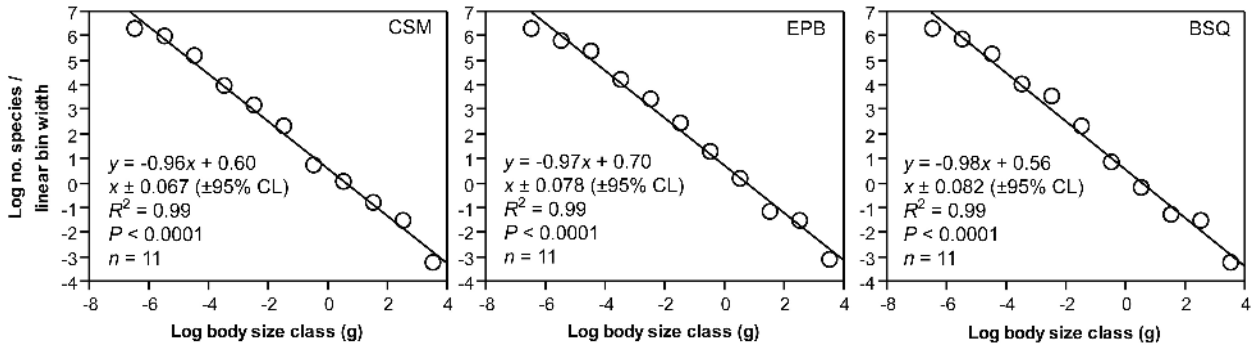

Fig. S2. Logged number of species per log body-size bin divided by linear bin-width versus the mid-point of the log size bin, for each estuary.
The almost isometric scaling indicates that species mean body-size distributions only slightly influence the predicted scaling exponents. The results are depicted for each of the three estuaries and are essentially indistinguishable. Fitting a truncated Pareto distribution to the cdf of species body sizes supported the estimates derived in A-C (*11*).

SOM Tables

Table S1. The number of species by animal group from the estuarine food webs used in analyses.[a]

	Estuary[b]				
Animal Group	CSM	EPB	BSQ	Pooled Species[c]	Pooled life stages[d]
Birds	39 / 43	42 / 45	39 / 41	64 / 70	64 / 70
Fishes	9 / 11	13 / 19	8 / 13	18 / 25	18 / 25
Invertebrates[e]	28 / 41	46 / 60	37 / 47	83 / 96	83 / 130
Parasites	42 / 47	61 / 65	46 / 48	79 / 85	101 / 129
Sums	118 / 142	162 / 189	130 / 149	244 / 276	266 / 354

a: Numbers before slash represent the number of species with high-quality abundance data used in *N* vs. *M* analyses. Numbers after slash represent the greater species number we were able to use in *L* vs. *M* analysis (*11*).

b: CSM = Carpinteria Salt Marsh; EPB = Estero de Punta Banda; BSQ = Bahía de San Quintín

c: The number of quantified species in the data pooled for the three estuaries. The before slash total free-living species is 165, after slash is 191.

d: For some species with complex life cycles, where stages have distinct morphology, body sizes, and trophic relationships, we separately treated the distinct stages in analyses. Excluding extra stages did not influence our findings concerning abundance scaling (*11*).

e: Free-living invertebrates.

Table S2. Summary statistics from general linear models explaining logged observed abundance using log body size (*M*) for parasitic and free-living animals in three estuaries.[a]

Estuary[b]	Effect	DF	SS	*F*-ratio	R^2	*P*
CSM	log body size (*M*)	1	407.0	193.4		<0.0001
	free-living or parasite	1	29.6	14.1		0.0003
	log *M* x free-living or parasite	1	54.0	25.6		<0.0001
	full model	3	792.9	125.6	0.74	<0.0001
	residual	131	275.8			
EPB	log body size (*M*)	1	394.5	198.7		<0.0001
	free-living or parasite	1	10.5	5.3		0.0227
	log *M* x free-living or parasite	1	76.0	38.3		<0.0001
	full model	3	966.3	162.2	0.74	<0.0001
	residual	174	345.4			
BSQ	log body size (*M*)	1	438.4	300.7		<0.0001
	free-living or parasite	1	11.9	8.2		0.0049
	log *M* x free-living or parasite	1	53.7	36.8		<0.0001
	full model	3	1024.0	234.1	0.83	<0.0001
	residual	143	208.5			

a: Statistics pertain to data in Fig. 1A-C

b: CSM = Carpinteria Salt Marsh; EPB = Estero de Punta Banda; BSQ = Bahía de San Quintín

Table S3. Parameter estimates from general linear models (Table S2) explaining logged observed abundance using log body size (*M*) for parasitic and free-living animals in three estuaries.

Estuary[a]	Parameter[b, c, d]	Estimate	SE	*t*	*P*
CSM	intercept	2.32	0.23	9.92	<0.0001
	log body size (*M*)	-1.00	0.07	-13.91	<0.0001
	free-living or parasite (f or p)	0.80	0.21	3.75	0.0003
	(log *M* + 0.83) x (f or p)	-0.36	0.07	-5.06	<0.0001
EPB	intercept	2.49	0.20	12.16	<0.0001
	log body size (*M*)	-0.89	0.06	-14.10	<0.0001
	free-living or parasite (f or p)	0.38	0.17	2.30	0.0227
	(log *M* + 1.13) x (f or p)	-0.39	0.06	-6.19	<0.0001
BSQ	intercept	2.28	0.18	12.53	<0.0001
	log body size (*M*)	-0.93	0.05	-17.34	<0.0001
	free-living or parasite (f or p)	0.41	0.14	2.86	0.0049
	(log *M* + 1.23) x (f or p)	-0.33	0.05	-6.07	<0.0001

a: CSM = Carpinteria Salt Marsh; EPB = Estero de Punta Banda; BSQ = Bahía de San Quintín

b: Parameter estimates for categorical effects represent the mean across effect levels (add the estimate for the first listed level, subtract for the second).

c: Continuous effects in interactions are centered on their means (*46, 47*).

d: We provide a worked example: the formula for the expected log abundance of CSM parasites is
$N = 2.32 - 1 \log M - 0.80 - (-0.36)(\log M + 0.83)$
$N = 1.52 - 1 \log M + 0.36 \log M + 0.30$
$N = 1.82 - 0.64 \log M$, which simplifies to the equation in Fig. 1A, with a rounding error explaining the -0.63 versus -0.64 slope.

Table S4. Summary statistics from general linear models explaining logged temperature-corrected abundance using log body size and trophic level for parasitic and free-living animals in three estuaries.[a, b]

Estuary[c]	Effect	DF	SS	*F*-ratio	R^2	*P*
CSM	log body size	1	606.1	402.5		<0.0001
	trophic level	1	127.6	84.7		<0.0001
	full model	2	671.2	222.9	0.77	<0.0001
	residual	132	198.8			
EPB	log body size	1	719.2	431.8		<0.0001
	trophic level	1	128.6	77.2		<0.0001
	full model	2	814.8	244.6	0.74	<0.0001
	residual	175	291.5			
BSQ	log body size	1	638.3	566.1		<0.0001
	trophic level	1	113.7	100.8		<0.0001
	full model	2	855.4	379.3	0.84	<0.0001
	residual	144	162.4			

a: Statistics pertain to data in Figs. 1G-I (which plot N_{temp} vs. log *M* at the mean *L* for each estuary: CSM 1.9, EPB 1.8, BSQ 1.9) and 3A-C (which plot N_{temp} vs. *L* at the mean log *M* for each estuary: CSM: -0.83, EPB: -1.13, BSQ: -1.23)

b: Models incorporating "free-living or parasite" and their interaction with log body size were never substantially or significantly better fit than those without those terms: CSM $F_{2,130}$= 2.2, P = 0.11; EPB $F_{2,173}$= 3.0, P = 0.053; CSM $F_{2,142}$= 0.65, P = 0.52. The marginal non-significance at EPB was associated with a weak effect (partial R^2 = 0.033).

c: CSM = Carpinteria Salt Marsh; EPB = Estero de Punta Banda; BSQ = Bahía de San Quintín

Table S5. Parameter estimates from general linear model (Table S4) explaining logged temperature-corrected abundance using log body size and trophic level for parasitic and free-living animals in three estuaries.

Estuary[a]	Parameter	Estimate	SE	*t*	*P*
CSM	intercept	5.51	0.39	14.10	<0.0001
	log body size	-0.74	0.04	-20.06	<0.0001
	trophic level	-1.80	0.20	-9.20	<0.0001
EPB	intercept	4.97	0.34	14.54	<0.0001
	log body size	-0.77	0.04	-20.78	<0.0001
	trophic level	-1.56	0.18	-8.79	<0.0001
BSQ	intercept	5.02	0.31	16.35	<0.0001
	log body size	-0.77	0.03	-23.79	<0.0001
	trophic level	-1.53	0.15	-10.04	<0.0001

a: CSM = Carpinteria Salt Marsh; EPB = Estero de Punta Banda; BSQ = Bahía de San Quintín

Table S6. Summary statistics from generalized linear models explaining trophic level using log body size for parasitic and free-living animals in three estuaries.[a]

Estuary[b]	Effect	DF	X^2	P
CSM	log body size (M)	1	12.0	0.0005
	parasite or free-living	1	89.1	<0.0001
	log M x parasite or free-living	1	48.7	<0.0001
	full model	3	212.6	<0.0001
	overdispersion (12.5)	189	2355.7	<0.0001
EPB	log body size (M)	1	23.0	<0.0001
	parasite or free-living	1	183.3	<0.0001
	log M x parasite or free-living	1	96.2	<0.0001
	full model	3	459.4	<0.0001
	overdispersion (8.8)	247	2182.3	<0.0001
BSQ	log body size (M)	1	27.2	<0.0001
	parasite or free-living	1	145.1	<0.0001
	log M x parasite or free-living	1	99.8	<0.0001
	full model	3	389.2	<0.0001
	overdispersion (9.1)	195	1782.4	<0.0001

a: Generalized linear models pertain to Fig. 2 A-C and used a $\log_e$-link, a Poisson error distribution with an overdispersion parameter, and trophic level data multiplied by 100 ("centitrophic" level) and rounded to have whole numbers appropriate for Poisson regression.

b: CSM = Carpinteria Salt Marsh; EPB = Estero de Punta Banda; BSQ = Bahía de San Quintín

Table S7. Parameter from generalized linear models (Table S6) explaining trophic level using log body size for parasitic and free-living animals in three estuaries.

Estuary[a]	Parameter[b, c, d]	Estimate	SE	X^2	P
CSM	intercept	5.22	0.03	9661.66	<0.0001
	log body size (M)	0.03	0.01	12.02	0.0005
	free-living or parasite (f or p)	-0.26	0.03	89.08	<0.0001
	(log M + 1.50) x (f or p)	0.06	0.01	48.75	<0.0001
EPB	intercept	5.18	0.03	16041.89	<0.0001
	log body size (M)	0.04	0.01	23.01	<0.0001
	free-living or parasite (f or p)	-0.28	0.02	183.32	<0.0001
	(log M + 1.71) x (f or p)	0.07	0.01	96.17	<0.0001
BSQ	intercept	5.20	0.03	13208.58	<0.0001
	log body size (M)	0.04	0.01	27.21	<0.0001
	free-living or parasite (f or p)	-0.27	0.02	145.06	<0.0001
	(log M + 1.70) x (f or p)	0.08	0.01	99.81	<0.0001

a: CSM = Carpinteria Salt Marsh; EPB = Estero de Punta Banda; BSQ = Bahía de San Quintín

b: Parameter estimates for categorical effects represent the mean across effect levels (add the estimate for the first listed level, subtract for the second).

c: Continuous effects in interactions are centered on their means (*46, 47*).

d: We provide a worked example: the formula for the expected trophic level of CSM parasites = [e^(5.22 + 0.03 log M - (-0.26) - 0.06 (log M + 1.50))] / 100. It is necessary to divide by 100 to convert "centitrophic level" units to trophic level.

Table S8. Summary statistics from generalized linear models explaining trophic level using log body size (with quadratic term) for the pooled parasitic and free-living animals in three estuaries.[a]

Estuary[b]	Effect	DF	X^2	P
CSM	log body size (M)	1	5.0	0.0247
	log M x log M	1	15.2	<0.0001
	full model	2	16.6	0.0002
	overdispersion (22.4)	190	4250.8	<0.0001
EPB	log body size (M)	1	10.2	0.0014
	log M x log M	1	38.3	<0.0001
	full model	2	38.6	<0.0001
	overdispersion (20.4)	248	5058.6	<0.0001
BSQ	log body size (M)	1	2.6	0.1049
	log M x log M	1	29.1	<0.0001
	full model	2	30.8	<0.0001
	overdispersion (22.2)	196	4359.4	<0.0001

a: Generalized linear models pertain to Fig. 2A-C and used a $\log_e$-link, a Poisson error distribution with an overdispersion parameter, and trophic level data multiplied by 100 ("centitrophic" level) to have whole numbers appropriate for Poisson regression.

b: CSM = Carpinteria Salt Marsh; EPB = Estero de Punta Banda; BSQ = Bahía de San Quintín

Table S9. Parameter estimates for generalized linear models (Table S8) explaining trophic level using log body size (with quadratic term) for the pooled parasitic and free-living animals in three estuaries.

Estuary[a]	Parameter[b]	Estimate	SE	X^2	P
CSM	intercept	5.13	0.05	6934.84	0.00
	log body size (M)	-0.02	0.01	5.04	0.02
	(log M + 1.50) x (log M + 1.50)	0.01	0.00	15.17	<0.0001
EPB	intercept	5.04	0.04	9305.00	0.00
	log body size (M)	-0.03	0.01	10.17	0.00
	(log M + 1.71) x (log M + 1.71)	0.02	0.00	38.31	<0.0001
BSQ	intercept	5.08	0.05	6812.72	0.00
	log body size (M)	-0.02	0.01	2.63	0.10
	(log M + 1.70) x (log M + 1.70)	0.02	0.00	29.10	<0.0001

a: CSM = Carpinteria Salt Marsh; EPB = Estero de Punta Banda; BSQ = Bahía de San Quintín

b: Continuous effects in interactions are centered on their means (*46, 47*).

Table S10. Summary statistics from general linear models explaining logged population production using log body size and trophic level for parasitic and free-living animals in three estuaries.[a]

Estuary[b]	Effect	DF	SS	*F*-ratio	R^2	*P*
CSM	log body size	1	0.2	0.1		0.7322
	trophic level	1	127.6	84.7		<0.0001
	full model	2	131.4	43.6	0.40	<0.0001
	residual	132	198.8			
EPB	log body size	1	0.6	0.3		0.5651
	trophic level	1	128.6	77.2		<0.0001
	full model	2	128.6	38.6	0.31	<0.0001
	residual	175	291.5			
BSQ	log body size	1	0.3	0.3		0.5808
	trophic level	1	113.7	100.8		<0.0001
	full model	2	118.8	52.7	0.42	<0.0001
	residual	144	162.4			

a: Statistics pertains to data in Fig. 4A-C.

b: CSM = Carpinteria Salt Marsh; EPB = Estero de Punta Banda; BSQ = Bahía de San Quintín

Table S11. Parameter estimates from general linear models (Table S10) explaining logged population production using log body size and trophic level for parasitic and free-living animals in three estuaries.

Estuary[a]	Parameter	Estimate[b]	SE	*t*	*P*
CSM	intercept	5.69	0.39	14.57	<0.0001
	log body size	0.01	0.04	0.34	0.73
	trophic level	-1.80	0.20	-9.20	<0.0001
EPB	intercept	5.25	0.34	15.35	<0.0001
	log body size	-0.02	0.04	-0.58	0.57
	trophic level	-1.56	0.18	-8.79	<0.0001
BSQ	intercept	5.24	0.31	17.06	<0.0001
	log body size	-0.02	0.03	-0.55	0.58
	trophic level	-1.53	0.15	-10.04	<0.0001

a: CSM = Carpinteria Salt Marsh; EPB = Estero de Punta Banda; BSQ = Bahía de San Quintín

b: Note that the antilogs of the trophic level parameter estimates provide the trophic transfer efficiencies.

Additional SOM References.

33. A. Poole, F. Gill, Eds., *The birds of North America: life histories for the 21st century*, (American Ornithologists' Union/Academy of Natural Sciences of Philadelphia, 1992-2003).

34. D. A. Sibley, *The Sibley field guide to birds of western North America* (Knopf, New York, 2003).

35. R. F. Hechinger, K. D. Lafferty, F. T. Mancini III, R. R. Warner, A. M. Kuris, *Evol Ecol* **23**, 651 (2009).

36. R. J. Williams, N. D. Martinez, *Am Nat* **163**, 458 (2004).

37. R. J. Williams, S. Yoon, A. Boit. (Microsoft Research & Pacific Ecoinformatics and Computational Ecology Lab, Cambridge & Berkeley, 2010).

38. I. Yoon, R.J. Williams, E. Levine, S. Yoon, J.A. Dunne, N.D. Martinez, paper presented at the IS&T/SPIE Symposium on Electronic Imaging, Visualization and Data Analysis, 2004.

39. M. A. Montes-Hugo, S. Alvarez-Borrego, *Estuarine Coast Shelf Sci* **56**, 517 (2003).

40. J. A. Rosales Casián, Ph.D., Centro de investigación científica y de educación superior de Ensenada (1997).

41. J. T. Fingerut, C. A. Zimmer, R. K. Zimmer, *Biol Bull* **205**, 110 (2003).

42. E. P. Odum, *Fundamentals of ecology* (Saunders, Philadelphia, 1971).

43. M. Begon, J. L. Harper, C. R. Townsend, *Ecology: individuals, populations, and communities* (Sinauer Associates, Sunderland, Mass., 1986).

44. J. F. Gillooly, A. P. Allen, J. H. Brown, in *Ecological networks: linking structure to dynamics in food webs,* M. Pascual, J. A. Dunne, Eds. (Oxford Univ. Press, Oxford, 2006), pp. 209-222.

45. E. P. White, B. J. Enquist, J. L. Green, *Ecology* **89**, 905 (2008).

46. M. H. Kutner, C. J. Nachtsheim, J. Neter, W. Li, *Applied linear statistical models* (McGraw-Hill/Irwin, Boston, ed. 5th, 2005).

47. G. P. Quinn, M. J. Keough, *Experimental design and data analysis for biologists* (Cambridge Univ. Press, Cambridge, UK, 2002).

48. P. H. Harvey, in *Scaling in Biology,* J. H. Brown, G. B. West, Eds. (Oxford Univ. Press, Oxford, 2000), pp. 253-265.